

## Bioactivation of Metal Oxide Surfaces. 1. Surface Characterization and Cell Response

Alireza Rezania,<sup>†,‡</sup> Robert Johnson,<sup>§</sup> Anthony R. Lefkow,<sup>||</sup> and Kevin E. Healy<sup>\*,†,‡</sup>

Division of Biological Materials, Northwestern University, 311 East Chicago Avenue, Chicago, Illinois 60611-3008; Department of Biomedical Engineering, Robert R. McCormick School of Engineering and Applied Science, Northwestern University, Evanston, Illinois 60201; Abbott Laboratories, Abbott Park, Illinois; and Basic Industrial Research Laboratory (B. I. R. L.), Northwestern University, Evanston, Illinois 60201

Received January 11, 1999. In Final Form: June 10, 1999

Silicon and titanium oxide surfaces (SiO<sub>2</sub>/Si and TiO<sub>2</sub>/Ti) were covalently modified with bioactive molecules (e.g., peptides) in a simple three-step procedure. Bioactive surfaces were synthesized by first immobilizing *N*-(2-aminoethyl)-3-aminopropyl-trimethoxysilane (EDS) to either polished quartz disks, polished silicon wafers, or sputter-deposited titanium films. Subsequently, a maleimide-activated surface amenable to tethering molecules with a free thiol (e.g., cysteine) was created by coupling sulfo-succinimidyl 4-(*N*-maleimidomethyl) cyclohexane-1-carboxylate (sulfo-SMCC) to the terminal amine on EDS. In particular, Cys-Gly-Gly-Asn-Gly-Glu-Pro-Arg-Gly-Asp-Thr-Tyr-Arg-Ala-Tyr (-RGD-) and Cys-Gly-Gly-Phe-His-Arg-Arg-Ile-Lys-Ala (-FHRRIKA-) peptides with terminal cysteine residues were immobilized on maleimide-activated oxides. X-ray photoelectron spectroscopy (XPS) and spectroscopic ellipsometry were used to assess the chemistry, thickness, and surface density of the grafted layers. EDS deposited from anhydrous methanol produced reaction site-limited monolayers (~0.28 nmol/cm<sup>2</sup>). Coupling of the sulfo-SMCC cross-linker (~0.03 nmol/cm<sup>2</sup>) and peptides (~0.004 nmol/cm<sup>2</sup>) resulted in an order of magnitude drop in surface density for each stage of the reaction scheme. Peptide-modified surfaces with densities varying over 2 orders (0.01–4 pmol/cm<sup>2</sup>) of magnitude were synthesized to study the effect of the peptides on mammalian cell function. The adhesion and spreading of cells derived from mammalian bone, in contact with the peptide-modified surfaces, was dependent on the specific peptide sequence grafted in a concentration-dependent manner. The grafting scheme presented has generality in coupling thiol-specific molecules to silicon or titanium surfaces.

### Introduction

In the fields of biomaterials, biosensors, chromatography, and biotechnology, there is a broad need for coupling molecules to solid supports that render the material biologically functional. Many different classes of biomolecules such as antibodies, enzymes, plasma proteins, extracellular matrix proteins, growth factors, and peptide fragments have been immobilized on surfaces.<sup>1–9</sup> Ideally, immobilization of a biomolecule to a surface should take few steps, be applicable to an array of surfaces (e.g., polymers, metals, and ceramics), and provide stable and functional molecular films with a high surface density to improve in situ performance.<sup>1</sup>

Immobilization of biological molecules is usually achieved by either physisorption or chemisorption techniques. Deposition of proteins, peptides, or enzymes on solid supports such as silica may be obtained by simply incubating the surface with the desired organic molecules. However, such a crude strategy results in surfaces which suffer from denaturation, leaching and inconsistency in the activity of the adsorbed layer, and these problems lead to difficulties in both understanding structure–function relationships and accurate surface characterization of the adsorbed layer.<sup>1,2,10</sup> Chemisorption of biomolecules does not suffer from the aforementioned disadvantages and provides a durable linkage between the molecule and the surface.<sup>11</sup> For example, the detection of enterotoxin B by a surface-bound antibody was dependent on covalent grafting of the antibody to silica surfaces. Antibodies that were physisorbed were not well-structured and acted like insulators interfering with capacitance-based detection methods.<sup>3</sup>

Surface modification techniques such as silanization, plasma gas discharge, vapor deposition, UV light, photoinitiated polymerization, and ion beam etching have been used to provide reactive groups at the material surface for covalent immobilization of biomolecules.<sup>12–15</sup> The reactive groups (–SH, –COOH, –NH<sub>2</sub>, and –OH)

\* To whom correspondence should be addressed. Phone: (312) 503-4735. Fax: (312) 503-2440. E-mail: kehealy@nwu.edu.

<sup>†</sup> Division of Biological Materials.

<sup>‡</sup> Robert R. McCormick School of Engineering and Applied Science.

<sup>§</sup> Abbott Laboratories.

<sup>||</sup> B. I. R. L.

(1) Bhatia, S. K.; Shriver-Lake, L. C.; Prior, K. L.; Georger, J. H.; Calvert, J. M.; Bredehorst, R.; Ligler, F. S. *Anal. Biochem.* **1989**, *178*, 408–413.

(2) Massia, S. P.; Hubbell, J. A. *Anal. Biochem.* **1990**, *187*, 292–301.

(3) Billard, V.; Martlet, C.; Binder, P.; Therasse, J. *Anal. Chim. Acta* **1991**, *249*, 367–372.

(4) Bearinger, J. P.; Castner, D. G.; Healy, K. E. *J. Biomater. Sci., Polym. Ed.* **1998**, *9*, 629–652.

(5) James, C. D.; Davis, R. C.; Kam, L.; Craighead, H. G.; Isaacson, M.; Turner, J. N.; Shain, W. *Langmuir* **1998**, *14*, 741–744.

(6) Mandenius, C. F.; Welin, S.; Danielsson, B.; Lunström, I.; *Anal. Biochem.* **1984**, *137*, 106–114.

(7) Hong, H.-G.; Jiang, M.; Sliger, S. G.; Bohn, P. W. *Langmuir* **1994**, *10*, 153–158.

(8) Nilsson, K.; Larsson, P.-O. *Anal. Biochem.* **1983**, *134*, 60–72.

(9) Reginer, F. E.; Noel, R. *J. Chromatogr. Sci.* **1976**, *14*, 316–320.

(10) Delamar, E.; Sundarababu, G.; Biebucyk, H.; Michel, B.; Gerber, C.; Sigrist, H.; Wolf, H.; Ringsdorf, H.; Xanthopoulos, N.; Mathieu, H. J. *Langmuir* **1996**, *12*, 1997–2006.

(11) Turner, D. C.; Testoff, M. A.; Conrad, D. W.; Gaber, B. P. *Langmuir* **1997**, *13*, 4855–4860.

(12) Matsuda, T.; Sugawara, T. *J. Biomed. Mater. Res.* **1995**, *29*, 749–756.

(13) Bearinger, J. P.; Castner, D. G.; Gollidge, S. L.; Rezaia, A.; Hubchak, S.; Healy, K. E. *Langmuir* **1997**, *13*, 5175–5183.

may be used to graft the desired biomolecule either directly or through a cross-linker to the surface.<sup>1,4,12,16–22</sup> Introduction of these reactive groups has predominately occurred on polymer surfaces;<sup>2,23,24</sup> however, using either thiolate or silane chemistry one can functionalize metal and oxide surfaces with the same groups.<sup>1,25–29</sup> In particular, either amino- or thiol-terminated monolayers provide a convenient method for producing reactive oxide surfaces amenable for coupling active biomolecules.<sup>1,7,30</sup> Bhatia et al.<sup>1</sup> utilized a thiol-terminated silane (mercaptoethylmethylethoxysilane) and heterobifunctional cross-linkers to graft antibodies to silica surfaces. Hong and co-workers<sup>7,30</sup> modified this approach to include an amino-terminated silane and a heterobifunctional cross-linker (*N*-succinimidyl 6-maleimidocaproate) to produce oriented metalloprotein nanostructures on silicon wafers. In Hong et al.'s work, the synthetic route resulted in a more hydrolytically stable maleimide-terminated surface prior to the coupling of proteins with oriented thiol-containing cysteine residues. Similarly, Xiao et al.<sup>31,32</sup> employed a multilayer film of poly(3-aminopropyl)siloxane and a series of heterobifunctional cross-linkers to conjugate cysteine-containing peptides to sputter-deposited titanium films.

In this manuscript we report on a method similar to that described by Hong et al.<sup>7</sup> and Xiao et al.<sup>31,32</sup> for covalent grafting of thiol-specific molecules to metal oxide surfaces. The synthetic strategy involves chemisorption of an aminofunctional organosilane *N*-(2-aminoethyl)-3-aminopropyl-trimethoxysilane (EDS) to the oxide surface (i.e., quartz, SiO<sub>2</sub>, or TiO<sub>2</sub>) and modifying the terminal amine with the heterobifunctional cross-linker sulfosuccinimidyl 4-(*N*-maleimidomethyl) cyclohexane-1-carboxylate (sulfo-SMCC) to produce maleimide-functional surfaces. As shown previously,<sup>7,22,30–32</sup> molecules with available thiols (e.g., peptides, proteins, antibodies, enzymes, polysaccharides, DNA, etc.) can be coupled to the maleimide-terminated substrate in both aqueous and non-

aqueous environments. Here, we report on the chemistry, indices of refraction, and the surface density of each immobilized layer determined by either X-ray photoelectron spectroscopy or spectroscopic ellipsometry. The synthetic route presented in this manuscript and others<sup>7,22,30–32</sup> ensures that the molecule is covalently linked to the substrate via the single thiol group present, thus allowing the rest of the molecule to freely interact with the ambient (e.g., enzyme substrates, antibody antigens, receptors on the surfaces of mammalian cells, etc.). The thiol-specific coupling strategy also enables accurate construction of a model molecular system which could be studied using molecular mechanics and dynamics of the modified surface.<sup>33</sup> Furthermore, the immobilization scheme allowed the synthesis of stable bioactive monolayers with a wide range of surface densities, thus allowing the study of the effect of ligand surface density on biological activity of the surface.<sup>34</sup>

## Experimental Section

**Sample Preparation.** Surface modifications were performed on polished quartz, silicon wafers (SiO<sub>2</sub>/Si), and sputter-deposited titanium surfaces (TiO<sub>2</sub>/Ti). Silicon samples were used for development of the immobilization protocol and subsequent surface characterization. Both polished quartz and SiO<sub>2</sub>/Si substrates were cleaned identically in the following manner. Polished quartz disks (Quartz Scientific Inc., Fairport Harbor, Ohio) or silicon wafers (n type, <100>, International Wafer Service, Portola Valley, CA) were cleaned ultrasonically for 10 min with ASTM Grade I water (resistivity 18 MΩ·cm: further referred to in this paper as ultrapure water), acetone, and hexane, etched in 9:1 (v/v) sulfuric acid:hydrogen peroxide for 15 min, and further rinsed in ultrapure water (WARNING: the etching solution can react violently with organic materials and should be handled carefully). All samples were dried in a laminar flow fume hood (Class 100) and stored until further use. Prior to surface modification, samples were exposed to an oxygen plasma (March Plasmod, Concord, CA) set at 0.5 mmHg and 100 W for 5 min. Samples cleaned in this manner wet with water (e.g.,  $\theta_{\text{Adv}}^{\text{H}_2\text{O}} < 10^\circ$ ), indicating the hydroxylated nature of the oxide surface. Samples were then immediately placed in the (aminoalkyl)alkoxysilane solution as detailed below.

The titanium films were deposited on silicon wafers (n type, <100>) in a Materials Research (MRC 902M) in-line sputter-deposition system. Following the deposition, the TiO<sub>2</sub>/Ti films (~1 μm thick) were cleaned in the same manner as the silicon and quartz samples with the exception of the sulfuric acid:hydrogen peroxide step, dried in a laminar flow fume hood, and stored until further use. Upon exposure to ambient, titanium films spontaneously form a thin oxide predominantly composed of an oxygen deficient TiO<sub>2</sub>. Prior to surface modification, all TiO<sub>2</sub>/Ti samples were cleaned in an oxygen plasma chamber in a manner analogous to the silicon and quartz samples ( $\theta_{\text{Adv}}^{\text{H}_2\text{O}} < 10^\circ$ ), subsequently exposed to a passivating solution of 40% (v/v) HNO<sub>3</sub> in ultrapure water at 50 °C for 20 min, rinsed in 50 °C ultrapure water for 5 min, and then placed in boiling ultrapure water for 2 h.<sup>35,36</sup> Samples were then immediately modified as described below.

(14) Dunkirk, S. G.; Gregg, S. L.; Duran, L. W.; Monfils, J. D.; Haapala, J. E.; Clapper, J. A.; Amos, R. A.; Guire, P. E. *J. Biomater. Appl.* **1991**, *6*, 131–156.

(15) Sheu, M.-S.; Hoffman, A. S.; Feijen, J. *J. Adhes. Sci. Technol.* **1992**, *6*, 995–1101.

(16) Trens, P.; Denoyel, R.; Rouquerol, J. *Langmuir* **1995**, *11*, 551–554.

(17) Massia, S. P.; Hubbell, J. A. *J. Biol. Chem.* **1992**, *267*, 10133–10141.

(18) Österberg, E.; Bergström, K.; Holmberg, K.; Schuman, T. P.; Riggs, J. A.; Burns, N. L.; Van Alstine, J. M.; Harris, J. M. *J. Biomed. Mater. Res.* **1995**, *29*, 741–747.

(19) Healy, K. E.; Lom, B.; Hockberger, P. E. *Biotech. Bioeng.* **1994**, *43*, 792–800.

(20) Margel, S.; Vogler, E. A.; Firment, L.; Watt, T.; Haynie, S.; Sogah, D. Y. *J. Biomed. Mater. Res.* **1993**, *27*, 1463–1476.

(21) Sukenik, C. N.; Balachander, N.; Culp, L. A.; Lewandowska, K.; Merritt, K. *J. Biomed. Mater. Res.* **1990**, *24*, 1307–1322.

(22) Rezania, A.; Thomas, C. H.; Branger, A. B.; Waters, C. M.; Healy, K. E. *J. Biomed. Mater. Res.* **1997**, *37*, 9–19.

(23) Drumheller, P. D.; Elbert, D. L.; Hubbell, J. A. *Biotechnol. Bioeng.* **1994**, *43*, 772–780.

(24) Beyer, D.; Matsuzawa, M.; Nakao, A.; Knoll, W. *Langmuir* **1998**, *14*, 3030–3035.

(25) Wasserman, S. R.; Tao, T.; Whitesides, G. M. *Langmuir* **1989**, *5*, 1074–1087.

(26) Wasserman, S. R.; Whitesides, G. M.; Tidswell, I. M.; Ocko, B. M.; Pershan, P. S.; Axe, J. D. *J. Am. Chem. Soc.* **1989**, *111*, 5822–5861.

(27) Tidswell, C. D.; Ertel, S. I.; Ratner, B. D.; Tarasevich, B. J.; Atre, S.; Allara, D. L. *Langmuir* **1997**, *13*, 3404–3413.

(28) Heid, S.; Effenberger, F. *Langmuir* **1996**, *12*, 2118–2120.

(29) Bain, C. D.; Whitesides, G. M. *J. Am. Chem. Soc.* **1988**, *110*, 3665–3666.

(30) Hong, H.-G.; Bohn, P. W.; Sliagar, S. G. *Anal. Chem.* **1993**, *65*, 1635–1638.

(31) Xiao, S.-J.; Textor, M.; Spencer, N. D.; Wieland, M.; Keller, B.; Sigrist, H. *J. Mater. Sci.: Mater. Med.* **1997**, *8*, 867–872.

(32) Xiao, S.-J.; Textor, M.; Spencer, N. D.; Sigrist, H. *Langmuir* **1998**, *14*, 5507–5516.

(33) Harbers, G. Computer-Aided Biomolecular Surface Engineering of Peptide Modified Materials. M.S. Thesis, Northwestern University, Chicago, IL, 1998.

(34) Rezania, A.; Healy, K. E. *Biotech. Progr.* **1999**, *15*, 19–32.

(35) Wisbey, A.; Gregson, P. J.; Peter, L. M.; Tuke, M. *Biomaterials* **1991**, *12*, 470–473.

(36) Healy, K. E.; Ducheyne, P. *J. Colloid Interface Sci.* **1992**, *150*, 404–417.

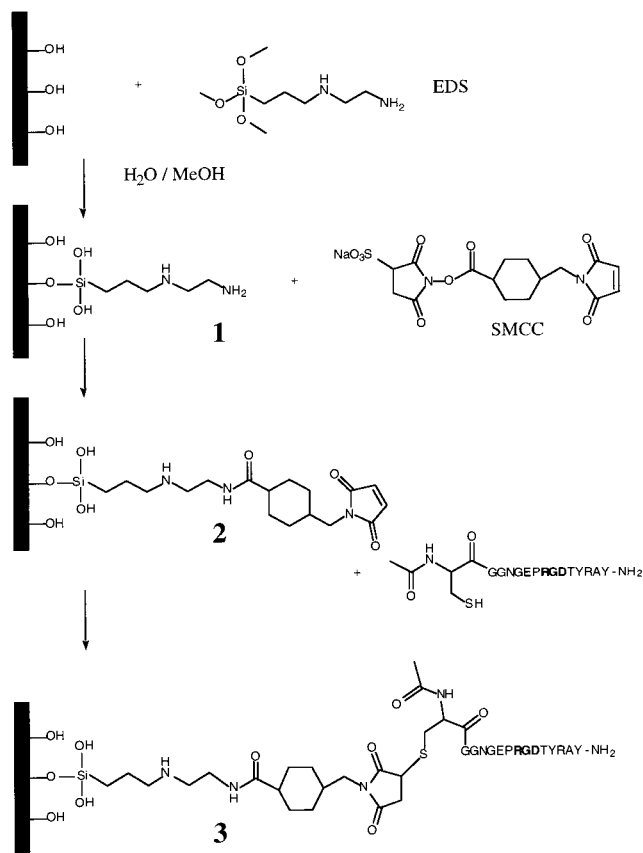


**Figure 1.** Reaction scheme (**1**, EDS; **2**, SMCC; **3**, peptide) for the surface modification of silicon, quartz, and titanium samples.

**Peptide Immobilization.** The immobilization scheme was developed to ensure that the coupling of the peptide occurred at an available thiol on the terminal cysteine of the molecule (Figure 1). Thus, all peptides used contained a terminal cysteine (C) with a double glycine (GG) spacer arm. Peptides were coupled to oxide surfaces in the following manner: *N*-(2-aminoethyl)-3-aminopropyl-trimethoxysilane (EDS) (Hüls America, Piscataway, NJ) was chemisorbed to cleaned and polished quartz disks, polished silicon wafers, or titanium films using modifications of methods published previously.<sup>37</sup> A solution of 1% EDS (v/v) and 94% anhydrous methanol (1 mM acetic acid in methanol) was prepared in a glovebox (nitrogen atmosphere). The solution was transferred into a laminar flow fume hood and 5% ultrapure water was added. The solution was mixed and the samples immersed for 5 min, rinsed three times in methanol, and baked in an oven for 5 min at 120 °C. The silanized samples were incubated in a 0.2 mM sulfo-SMCC solution (Pierce, Rockford, IL) prepared in 50 mM sodium borate buffer (pH = 7.5) for 30 min, followed by three rinses with 50 mM sodium borate buffer, and three rinses with ultrapure water. The maleimide-terminated surfaces were incubated for 20 h at 4 °C in a 160  $\mu$ M peptide solution prepared in 0.1 M sodium phosphate buffer (pH = 6.6). Peptide surfaces with different RGD surface densities were also prepared by using input peptide concentrations of 160, 1.6, 0.016, and 0.00016  $\mu$ M in 0.1 M sodium phosphate buffer (pH = 6.6). The samples were then removed from the peptide solution, rinsed three times with sodium phosphate buffer (0.1 M) followed by three rinses in ultrapure water, dried

in a laminar flow hood, and then stored in a desiccator until further analysis. The peptide sequences used were Ac-Cys-Gly-Gly-Gly-Asn-Gly-Pro-Arg-Gly-Asp-Thr-Tyr-Arg-Ala-Tyr-NH<sub>2</sub> (RGD-peptide), Ac-Cys-Gly-Gly-Phe-His-Arg-Arg-Ile-Lys-Ala-NH<sub>2</sub> (FHRRIKA-peptide), Ac-Cys-Gly-Gly-Asn-Gly-Glu-Pro-Arg-Gly-Glu-Thr-Tyr-Arg-Ala-Tyr-NH<sub>2</sub> (RGE-peptide), and Ac-Cys-Gly-Gly-Arg-Phe-His-Ala-Arg-Ile-Lys-NH<sub>2</sub> (RFHARIK-peptide). To reduce the reactivity of the peptides' end groups and degradation by exoproteases, the amino and carboxy termini were acetylated and amidated, respectively. The -RGD- or -FHRRIKA-based sequences are unique to bone sialoprotein, the major noncollagenous protein in bone matrix, and have been shown to interact with osteoblasts (cells that produce bone in vivo) through integrin- and proteoglycan-based engagement, respectively.<sup>34</sup> -RGE- and -RFHARIK- surfaces served as scrambled residue (inactive) controls of the active peptides. The peptides were synthesized and verified as >97% pure by HPLC and mass spectroscopy by TANA Laboratories (Houston, TX).

**Surface Characterization and Performance Methods.** *X-ray Photoelectron Spectroscopy Analysis.* XPS analyses were conducted on a Perkin-Elmer 5600 XPS/SIMS instrument with a monochromatic Al K $\alpha$  X-ray source (1486.6 eV) with a Omni Focus III small-area lens and a multichannel detector. A concentric hemispherical analyzer (CHA) was operated in the constant analyzer transmission mode to measure the binding energies of emitted photoelectrons. The binding energy scale was calibrated by the Au 4f<sub>7/2</sub> peak at 83.9 eV, and the linearity was verified by the Cu 3p<sub>1/2</sub> and Cu 2p<sub>3/2</sub> peaks at 76.5 and 932.5 eV, respectively. An electron flood gun was used and set between 4 and 7 eV to minimize charging. Survey spectra were collected from 0 to 1100 eV with a pass energy of 188 eV, and high-resolution spectra were collected for each element detected (e.g., C, N, O, Si, and Ti) with a pass energy of 23.5 eV. Survey and high-resolution spectra were collected at various takeoff angles, defined as the angle spanned by the electron path to the analyzer and the sample surface. All spectra were referenced by setting the hydrocarbon C 1s peak to 285.0 eV to compensate for residual charging effects. Data for percent atomic composition and atomic ratios were calculated using manufacturer-supplied sensitivity factors.

**Spectroscopic Ellipsometry Analysis.** Spectroscopic ellipsometry was used to determine the thickness and surface density of the immobilized molecules grafted to the silicon and titanium surfaces. A MOSS-Sopra (model ES4G) multilayer optical spectrometric scanner (Sopra, Inc., Acton, Ma), equipped with a high-pressure Xenon arc lamp (75 W) and a rotating polarizer was used to analyze the SiO<sub>2</sub> surfaces. Due to an upper cutoff of the photodetector, the range of the wavelengths used in this study was 250–900 nm. A J. A. Woollam spectroscopic ellipsometer (M44-STD model; Lincoln, NE) equipped with a rotating analyzer and a Xenon arc lamp (75 W) was used to analyze the TiO<sub>2</sub>-modified surfaces. The range of wavelengths used to analyze the titanium samples was 430–650 nm. A clean sample (silicon or titanium) was used as a reference to determine the oxide thickness (~2.4 nm for SiO<sub>2</sub>/Si and ~2 nm for TiO<sub>2</sub>/Ti). Samples during each stage of the immobilization were analyzed: typically, data were collected from at least two spots on each sample, and three to five samples were analyzed. Data were collected in air at room temperature (~25 °C) and relative humidity (~30–50%). The immobilized layers on either silicon or titanium substrates were assumed to be

(37) Healy, K. E.; Thomas, C. H.; Reznia, A.; Kim, J. E.; McKeown, P. J.; Lom, B.; Hockberger, P. E. *Biomaterials* **1996**, *16*, 195–208.

homogeneous, flat, optically isotropic, and transparent (i.e.,  $\kappa = 0$ ). The thickness and index of refraction of oxides or grafted layers were calculated by using the software provided with the ellipsometer. The experimental  $\psi$  and  $\Delta$  versus energy data were fit using a Cauchy model and a library of  $n$  versus wavelength data provided by the software was used to calculate the index of refraction and thickness of the layers. The quality of fits were considered to be acceptable if the calculated-mean-square error (MSE) values were less than 3, and typically the MSE values were around 0.01.

#### Cell Attachment to Peptide-Modified Surfaces.

Analysis of cell behavior on peptide modified surfaces (RGD and RGE) was performed with primary cultures of bone synthesizing cells, osteoblasts. Cells were isolated using previously described methods.<sup>37</sup> Cells derived from the primary culture were referred to as rat calvaria osteoblast-like (RCO). RCO cells were maintained in growth medium containing Dulbecco's modified Eagle's medium (DMEM; Gibco, Grand Island, NY), 15% heat-inactivated fetal bovine serum (FBS), 1% penicillin-streptomycin, 1% fungizone, Hepes buffer (15 mM), sodium pyruvate (1 mM), and ascorbic acid (5  $\mu$ g/mL). Isolated cells were characterized by alkaline phosphatase staining and Von Kossa staining for mineralization. The latter resulted in 75 cm<sup>2</sup> flasks that contained sheets of mineralized tissue.<sup>37</sup>

The effect of the peptide chemistry and surface density on RCO cell attachment was examined by measuring cell density (number of attached cells/cm<sup>2</sup>) using optical microscopy with digital image acquisition and analysis. RCO cells were seeded for 4 h on surfaces at a density of  $\sim 10^4$  cells/cm<sup>2</sup> in DMEM with BSA (1 mg/ml) at 37 °C. Following 4 h of incubation, the surfaces were rinsed three times with PBS, and the cells were fixed for 15 min in 4% formaldehyde in PBS at room temperature. The cell density was calculated by counting the number of attached cells per analyzed field (0.013 cm<sup>2</sup>) on a minimum of nine randomly chosen fields. Analyses of variance (ANOVA) with Neuman-Keuls post hoc comparisons were used to assess levels of significance. Cell spreading on the modified surfaces was assessed using RCO cells incubated for 4 h at a density of  $\sim 5 \times 10^3$  cells/cm<sup>2</sup> on control (RGE surfaces) and active peptide surfaces at 37 °C in DMEM with 1 mg/mL of BSA. The procedures for collecting images and image analysis are given elsewhere.<sup>38</sup> On each surface, five randomly chosen fields were imaged and  $\sim 100$ –200 cells/surface were examined. The area and number of attached cells to tissue culture plastic (TCPS) in the presence of 15% FBS in DMEM was used as a positive control.

## Results and Discussion

**Surface Chemistry.** XPS analyses of modified silicon wafers and titanium films confirmed changes in both the surface composition and chemistry consistent with the proposed reactions (Table 1). Survey spectra collected from oxygen plasma treated and passivated titanium samples indicated typical Ti 2p, Ti 3s, O 1s, C 1s, and O KLL and Ti LMM Auger peaks (Figure 2A–B). Analysis of survey spectra after silanation indicated an increase in N 1s intensity, and the presence of Si 2s and Si 2p peaks confirmed the immobilization of the silane to the hydroxylated surface (Figure 2C and Table 1). Water contact angle measurements ( $\theta_{Adv}^{H_2O} \approx 36^\circ$ ,  $\theta_{Rec}^{H_2O} < 10^\circ$ ) were consistent with a reaction-site limited monolayer of an

**Table 1. Atomic Surface Composition and N/Si Atomic Ratios for SiO<sub>2</sub>/Si and TiO<sub>2</sub>/Ti Surfaces Modified with EDS, SMCC, and –RGD– Peptide<sup>a</sup>**

modification (layer)	atomic composition <sup>b</sup>					atomic ratio N/Si
	%N	%O	%C	%Si	%Ti	
SiO <sub>2</sub> /Si	<0.5	45.1	8.2	46.2		
TiO <sub>2</sub> /Ti-passivated	1.6	47.4	31.5		19.6	
SiO <sub>2</sub> /Si + 1	1.7	40.0	17.5	40.4		
TiO <sub>2</sub> /Ti + 1	2.0	52.1	21.2	0.8	23.8	2.5
theoretical						2.0
SiO <sub>2</sub> /Si + 2	2.9	36.6	28.3	31.8		
TiO <sub>2</sub> /Ti + 2	2.4	51.4	25.4	0.8	20.0	3.0
theoretical						3.0
SiO <sub>2</sub> /Si + 3	4.2	35.0	28.6	32.2		
TiO <sub>2</sub> /Ti + 3	4.2	47.8	29.2	0.4	18.4	10.5
theoretical						26.0

<sup>a</sup> Data shown are averages of at least two to four specimens for each stage of the reaction scheme. <sup>b</sup> For a takeoff angle of 65°, defined as the angle spanned by the electron path to the analyzer and the surface of the sample.

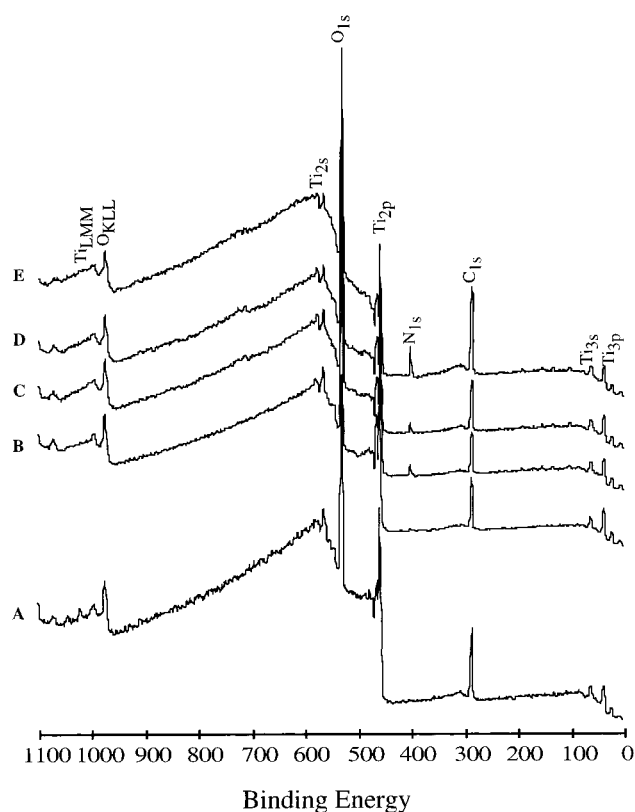


**Figure 2.** XPS survey spectra of clean (A), passivated (B), EDS (C), SMCC (D), and RGD peptide (E) on TiO<sub>2</sub>/Ti substrates. All surveys were normalized by the maximum O 1s signal at  $\sim 533.1$  eV in each spectrum.

amino-terminated surface.<sup>39</sup> High-resolution N 1s spectra indicated the amines existed as both free base, 399.3 eV, and protonated, 401.1 eV, with relative areas of 60 and 40%, respectively. Reaction of the heterobifunctional cross-linker (sulfo-SMCC) with the primary amine increased the N 1s and C 1s signals relative to the other peaks (Figure 2D). Immobilization of the peptide to the maleimide-terminated surface yielded substantial increases in both the N 1s and C 1s signals (Figure 2E). Survey spectra were qualitatively similar on the SiO<sub>2</sub>/Si and TiO<sub>2</sub>/Ti substrates (Figure 3) and reinforced the synthetic route.

(38) Thomas, C. H.; McFarland, C. D.; Jenkins, M. L.; Rezania, A.; Steele, J. G.; Healy, K. E. *J. Biomed. Mater. Res.* **1997**, *37*, 81–90.

(39) Stenger, D. A.; Georger, J. H.; Dulcey, C. S.; Hickman, J. J.; Rudolph, A. S.; Nielsen, T. B.; McCort, S. M.; Calvert, J. M. *J. Am. Chem. Soc.* **1992**, *114*, 8435–8442.

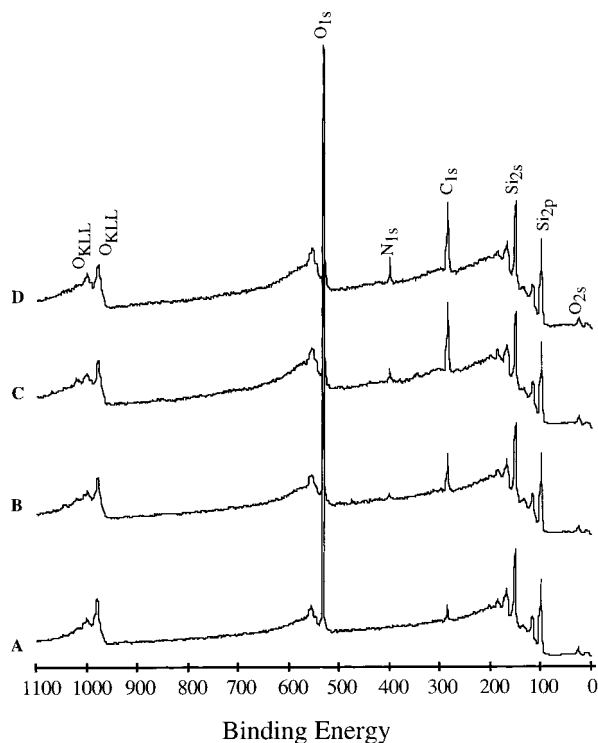


**Figure 3.** XPS surveys of clean (A), EDS (B), SMCC (C), and RGD peptide (D) surfaces on  $\text{SiO}_2/\text{Si}$  substrates. All surveys were normalized by the maximum O 1s signal at  $\sim 533.1$  eV in each spectrum.

The extent of the reaction scheme is more easily visualized by examination of the N 1s, Si 2p, C 1s, and Ti 2p high-resolution XPS spectra collected from  $\text{TiO}_2/\text{Ti}$  substrates (Figure 4). The most obvious differences were observed in the N 1s, C 1s, and Si 2p spectra. Clean titanium surfaces (Figure 4A) were absent of significant N 1s and Si 2p signals, but the C 1s signal at 285 eV displayed significant asymmetrical broadening and substantial  $\text{CH}_x$  content. The broad C 1s signal is consistently observed on Ti exposed to air and represents adsorption of ubiquitous species from the atmosphere.<sup>36,40</sup> N 1s signals were minimal on the passivated samples and were attributed to N incorporation into the Ti film during sputtering (Figure 4B and Table 1). The  $\text{Ti}^0$  2p<sub>3/2</sub> metal peak at 454 eV decreased relative to the  $\text{Ti}^{4+}$  2p<sub>3/2</sub> oxide peak at 457 eV, indicating the oxide became thicker due to the passivation. Upon silanation of the passivated surface, strong N 1s and Si 2p signals were observed (Figure 4C) and the C 1s signal area (i.e., line width) became smaller, leading to a lower relative C composition (Table 1). The lower C composition was probably due to the exchange of physisorbed species with the (aminoalkyl)-trialkoxysilane. Coupling SMCC to the surface led to a slight increase in the N 1s signal and attenuation of the Si 2p peak (Figure 4D). The most striking difference was observed for the C 1s peak in Figure 4D, which displayed a second peak at 288.5 eV associated with amide and carbonyl carbons in the SMCC. Chemisorption of the peptide enhanced the peak at 288.5 eV relative to the  $\text{CH}_x$  peak, which was indicative of an increase in the amide, carbonyl, and carboxylic acid carbons on the surface (Figure 4E). The N 1s peak also dramatically increased after coupling the peptide to the surface (Figure 4E). The Ti 2p peak was relatively unchanged due to the

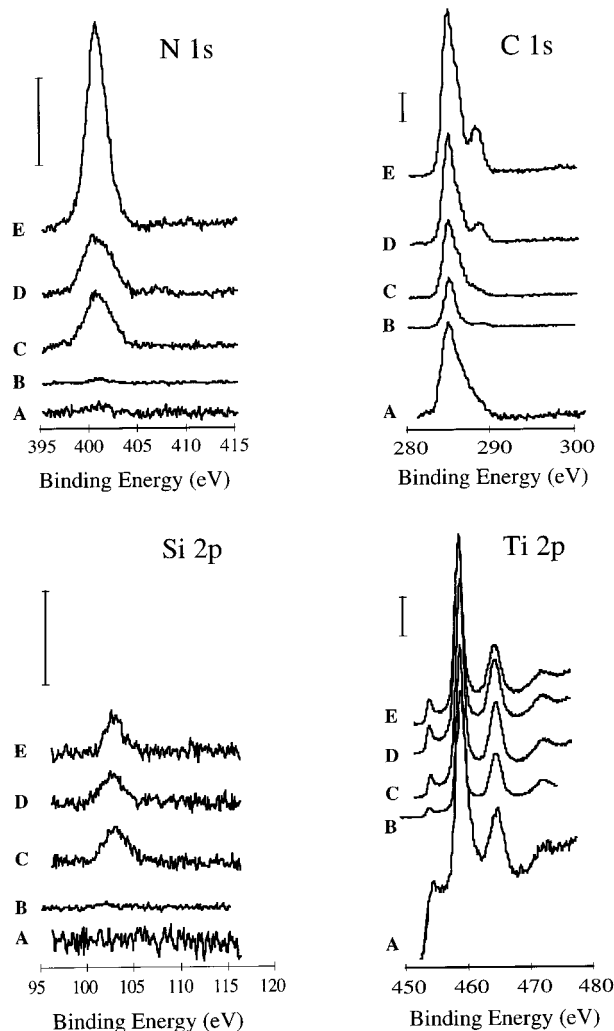


**Figure 4.** High-resolution XPS C 1s, N 1s, Si 2p, and Ti 2p spectra of clean (A), passivated (B), EDS (C), SMCC (D), and RGD peptide (E) on  $\text{TiO}_2/\text{Ti}$  substrates.

immobilization of the EDS, SMCC, and peptide. The N/Si ratios for each stage of the modification were 125%, 100%, and 40% of theoretical estimates for **1**, **2**, and **3**, respectively. A salient feature of the surface, based on the XPS measurements, was that the efficiency of coupling decreased upon subsequent modification, such that the peptide had the lowest atomic composition relative to theoretical values. The perceived reduction in grafting was based on a combination of the depth of analysis of XPS and lower surface density of the peptide, and the latter was further supported by the spectroscopic ellipsometry data discussed below.

**Monolayer Thickness and Index of Refraction.** Spectroscopic ellipsometry provided additional evidence of the extent of coupling for each layer on either substrate. Table 2 shows that the total thickness of the layer increased during each stage of the modification, and within experimental error, the thickness of each layer was consistent on each substrate. The silicon oxide thickness ( $\sim 2.4$  nm) was typical of a native oxide layer on silicon surfaces,<sup>25,41</sup> and the thickness of the titanium oxide ( $\sim 2$  nm) was consistent with previously reported values of 2–4 nm.<sup>40,42–44</sup> The thickness of the EDS layer ( $\sim 0.7$  nm)

(40) Sundgren, J.-E.; Bodo, P.; Lundstrom, I. *J. Colloid Interface Sci.* **1986**, *110*, 9–20.

(41) Carim, A. H.; Dovek, M. M.; Quate, C. F.; Sinclair, R.; Vorst, C. *Science* **1987**, *237*, 630–633.

(42) Lausmaa, J.; Mattsson, L.; Rolander, U.; Kasemo, B. *Mater. Res. Symp. Proc.* **1986**, *35*, 351.

**Table 2. Thickness, Molar Refractivities, Refractive Indices, and Surface Densities of Immobilized EDS, SMCC, and Peptide (RGD or FHRRIKA) Layers on SiO<sub>2</sub>/Si and TiO<sub>2</sub> Surfaces<sup>a</sup>**

layer	thickness (nm)	molar refractivity (cm <sup>3</sup> /mol)	refractive index $\lambda = 589.2$ nm	surface density (nmol/cm <sup>2</sup> )
EDS				
SiO <sub>2</sub> /Si <sup>b</sup>	0.67 ± 0.09	40.3	1.310 ± 0.020	0.281 ± 0.045
TiO <sub>2</sub> /Ti <sup>c</sup>	0.73 ± 0.07	40.3	1.326 ± 0.007	0.364 ± 0.028
SMCC				
SiO <sub>2</sub> /Si	0.40 ± 0.07	53.6	1.379 ± 0.050	0.031 ± 0.019
TiO <sub>2</sub> /Ti	0.37 ± 0.04	53.6	1.534 ± 0.004	0.075 ± 0.008
RGD peptide				
SiO <sub>2</sub> /Si	0.41 ± 0.05	376.0	1.440 ± 0.003	0.004 ± 0.001
TiO <sub>2</sub> /Ti	0.39 ± 0.01	376.0	1.656 ± 0.007	0.006 ± 0.001
FHRRIKA	0.27 ± 0.05	310.2	1.495 ± 0.010	0.006 ± 0.002
SiO <sub>2</sub> /Si				

<sup>a</sup> The thickness and molar refractivity values refer to each layer (EDS, SMCC, or peptide), and the refractive index values correspond to the composite layer(s). Measurements were made in triplicate. <sup>b</sup> The thickness and index of refraction of the SiO<sub>2</sub> oxide were ~2.6 nm and 1.461, respectively. <sup>c</sup> The thickness and index of refraction of the TiO<sub>2</sub> oxide were ~2.2 nm and 2.251, respectively.

was similar to that reported elsewhere<sup>37,39,45</sup> and was not indicative of a trans-extended chain (~1.2 nm), but was consistent with the concept that the finite number of accessible surface hydroxyl groups (~4–9 OH/nm<sup>2</sup>) on SiO<sub>2</sub>/Si<sup>46</sup> and TiO<sub>2</sub>/Ti<sup>47</sup> substrates limits the extent of the reaction and the close packing of the monolayer. Thus, the thickness can be modeled by a uniformly distributed and disordered monolayer that would have a refractive index (see below) of a complete monolayer but a smaller thickness.<sup>26</sup> Molecular mechanics and dynamics models of either EDS–TiO<sub>2</sub>/Ti or SiO<sub>2</sub>/Si surfaces predict thickness data within 10% of the experimental values<sup>33</sup> and support the uniformly distributed and disordered monolayer model. One may refer to these EDS layers as reaction-site limited monolayers,<sup>39,48</sup> to distinguish them from complete, close-packed monolayers as observed with alkanethiolates chemisorbed on gold, or intermediate length alkyltrichlorosilane films on silicon substrates.<sup>28,29,49</sup> The increases in thickness values for the SMCC- (~0.4 nm) and peptide-grafted (~0.4 nm) surfaces were consistent with additional layers on the EDS but were considerably less than extended chain projections for the respective layers. These thickness data can also be modeled by uniformly distributed and disordered monolayers as well.<sup>26,33</sup> As expected, the thickness of the shorter peptide (FHRRIKA; ~0.27 nm) was less than that of the RGD peptide.

The use of spectroscopic ellipsometry also allowed the estimation of the refractive index of each layer.<sup>50–52</sup> The measured indices of refraction values in Table 2 are composite measurements that include contributions from the underlying layer(s). The index of refraction for the EDS layer (~1.3) was less than the index of refraction of bulk EDS (~1.4). Previous ellipsometry studies have assumed refraction indices in the range of 1.4–1.44 (i.e., the index of refraction of bulk silane) as an estimate for

immobilized aminosilane layers on solid supports.<sup>25,26,39,45</sup> To our knowledge, there are no published reports on the index of refraction of (aminoalkyl)alkoxysilane layers immobilized on oxide surfaces via spectroscopic ellipsometry. However, Stenger et al.<sup>39</sup> assumed an effective index of refraction of ~1.35 for their EDS layer and reported a thickness measurement of ~5 Å. These data are consistent with our index of refraction and thickness values for the EDS film. On the basis of models of monolayers proposed by Wasserman et al.,<sup>25</sup> the index of refraction and thickness data support the proposed model of uniformly distributed and disordered monolayers of EDS. Molecular mechanics and dynamics studies also predicted a disordered monolayer.<sup>33</sup> The index of refraction data for the SMCC and peptide layers (RGD and FHRRIKA) were within the range expected for organic molecules and proteins, ~1.3 to 1.8, deposited on solid supports.<sup>53–55</sup> As with the EDS layer, the spectroscopic ellipsometry data led to the interpretation of the SMCC and peptide films as incomplete and diffuse monolayers. Higher refractive indices for SMCC and the peptides were measured on TiO<sub>2</sub>/Ti as compared to SiO<sub>2</sub>/Si substrates and were attributed to the composition of the molecule, a higher density of the initially bound EDS and subsequent molecules, and the surface roughness of the underlying substrates.

**Surface Density of Grafted Layers.** The surface density of each layer was estimated using the Lorentz–Lorenz equation and relating the optical constants, thickness, and surface density as follows:

$$\left(\frac{n^2 - 1}{n^2 + 2}\right) = 0.01 \left[ \frac{A_1 \Gamma_1}{d_1} + \frac{A_2 \Gamma_2}{d_2} + \dots \right] \quad (1)$$

where  $n$  is the real component of the refractive index of the combined layer(s),  $A$  (cm<sup>3</sup>/mol) is the molar refractivity of the adsorbed layer,  $d$  (nm) is the thickness of the layer, and  $\Gamma$  (nmol/cm<sup>2</sup>) is the surface density of the immobilized layer. The molar refractivity of each molecular layer was calculated by using the mean-bond refractivity values for sodium D light ( $\lambda = 589.2$  nm) and assuming that each layer was planar.<sup>56</sup> Table 2 shows the surface density values obtained from spectroscopic ellipsometry on SiO<sub>2</sub>/Si and TiO<sub>2</sub>/Ti surfaces. The surface density of the EDS film (~0.3 nmol/cm<sup>2</sup> or 55 Å<sup>2</sup>/molecule) was consistent

(43) Lausmaa, J.; Kasemo, B.; Rolander, U.; Bjursten, L. M.; Ericson, L. E.; Rosander, L.; Thomsen, P. *Preparation, Surface Spectroscopic and Electron Microscopic Characterization of Titanium Implant Materials*; Ratner, B. D., Ed.; Elsevier Science Publishers, B. V.: Amsterdam, 1988; pp 161–174.

(44) Callen, B. W.; Lowenberg, B. F.; Lugowski, S.; Sodhi, R. N. S.; Davies, J. E. *J. Biomed. Res.* **1995**, *29*, 279–290.

(45) Moon, J. H.; Shin, J. W.; Kim, S. Y.; Park, J. W. *Langmuir* **1996**, *12*, 4621–4624.

(46) Zhuravlev, L. T. *Langmuir* **1987**, *3*, 316–318.

(47) Healy, K. E.; Ducheyne, P. *Biomaterials* **1992**, *13*, 553–61.

(48) Durfor, C. N.; Turner, D. C.; Georger, J. H.; Peek, B. M.; Stenger, D. A. *Langmuir* **1994**, *10*, 148–152.

(49) Bierbaum, K.; Kinzler, M.; Woll, C.; Grunze, M. *Langmuir* **1995**, *11*, 512–518.

(50) Aspens, D. E. *J. Vac. Sci. Technol.* **1981**, *18* (2), 289–295.

(51) Aspens, D. E. *Thin Solid Films* **1993**, *233*, 1–8.

(52) Aspens, D. E. *Proc. SPIE-Int. Soc. Opt. Eng.* **1988**, *946*, 84–97.

(53) Arwin, H.; Martensson, J.; Lundstrom, I. *Appl. Phys. Commun.* **1992**, *11* (1), 41–48.

(54) Martensson, J.; Arwin, H. *Langmuir* **1995**, *11*, 963–968.

(55) Cuypers, P. A.; Corsel, J. W.; Janssen, M. P.; Kop, J. M. M.; Hermens, W. T.; Henker, H. C. *J. Biol. Chem.* **1983**, *258*, 2426–2431.

(56) Vogel, A. I.; Cresswell, W. T.; Leicester, J. *J. Phys. Chem.* **1954**, *58*, 174–177.

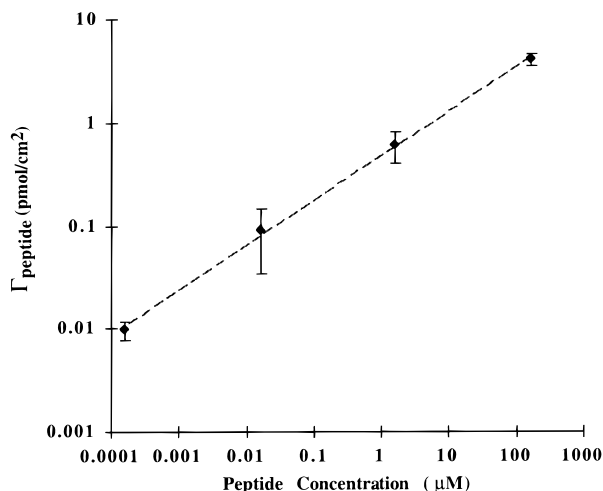


**Figure 5.** Surface density (pmol/cm<sup>2</sup>) of RGD grafted to silicon surfaces as a function of input peptide concentration (μM). Three samples per input concentration were used. The dotted line represents a linear regression fit with a slope and intercept of 0.433 and -0.325, respectively.

with previously reported surface density values (0.2–0.4 nmol/cm<sup>2</sup>) of thin aminosilane layers on silicon oxide surfaces.<sup>16,31,32,45,57–60</sup> A theoretical monolayer of EDS, which neglects any steric influence, has a maximum surface density of ~0.8 nmol/cm<sup>2</sup>, assuming a hydroxyl surface density of ~1 OH/20 Å<sup>2</sup>.<sup>46</sup> The efficiency of EDS immobilization was higher on TiO<sub>2</sub> surfaces than on the SiO<sub>2</sub> surfaces, which corresponded to ~46% and ~35% of the surface hydroxyls occupied, respectively. These data point to a reaction-site limited monolayer of EDS on metal oxides, where only ~40% of the surface hydroxyls are occupied. Molecular modeling of EDS monolayers formed by chemisorption with the basic hydroxyls on a TiO<sub>2</sub>(110) surface showed a well-packed but disordered layer consistent with the aforementioned data.<sup>33</sup> The surface density of the SMCC layer (~0.03–0.08 nmol/cm<sup>2</sup>) on the oxides was 1 order of magnitude lower than the EDS layer; similarly, the surface density of the peptide layers (~0.004–0.006 nmol/cm<sup>2</sup>) was 1 order of magnitude less than the SMCC layer (Table 2). These data support the reduction in coupling efficiency for each progressive stage of the reaction as identified by the XPS measurements. Although the surface density of the EDS molecules (Tables 2) on SiO<sub>2</sub> and TiO<sub>2</sub> oxides were similar, large differences were observed for the SMCC layer. Such differences were attributed to the surface roughness of the oxides, and reaction efficiencies of the grafted layers. The surface density of peptide surfaces prepared using different concentrations (0.00016–160 μM) of solution-phase RGD was also calculated. At the largest input peptide concentration (160 μM), the grafted surface density was 4 pmol/cm<sup>2</sup> (Figure 5), suggesting that the peptide was coupled to one out of approximately eight SMCC sites (surface density of SMCC was ~31 pmol/cm<sup>2</sup>). Xiao et al.<sup>31,32</sup> made similar observations regarding both low and diminishing reaction efficiency when coupling cysteine-terminated peptides to maleimide-activated surfaces synthesized with SMCC. In addition, they observed that the final thioether formation was dependent on the molecular size of the peptide.<sup>32</sup> Thus, the difference in the coupling yield of the

**Table 3. Mean Areas and Percentage of Attached RCO Cells on -RGD- and -RGE- Grafted Surfaces following 4 h of Incubation in the Presence of 1% BSA in DMEM<sup>a</sup>**

surface	mean cell area ± SD (μm) <sup>2</sup> <sup>b</sup>	% cell attached <sup>c</sup>
-RGD- (4 ± 1 pmol/cm <sup>2</sup> )	2,342 ± 669 <sup>d</sup>	88 ± 7
-RGD- (0.62 ± 0.25 pmol/cm <sup>2</sup> )	2,527 ± 600 <sup>d</sup>	78 ± 7
-RGD- (0.01 ± 0.002 pmol/cm <sup>2</sup> )	433 ± 171	29 ± 7 <sup>e</sup>
-RGE- (4 ± 1 pmol/cm <sup>2</sup> )	489 ± 155	23 ± 7 <sup>e</sup>
TCPS + FBS	2,286 ± 1126 <sup>d</sup>	

<sup>a</sup> Cell attachment to TCPS in the presence of 15% FBS was used as positive control. <sup>b</sup> Three samples and 100–200 cells per surface were examined. <sup>c</sup> The number of attached cells were normalized to number of attached cells to TCPS in the presence of 15% FBS. <sup>d</sup> Samples are significantly higher than the other surfaces (ANOVA, Neuman–Keuls test, *p* < 0.01). <sup>e</sup> Samples are significantly less than others (ANOVA, Neuman–Keuls test, *p* < 0.01).

cysteine-terminated peptides in this work (15 amino acids) and that of Xiao's (4 and 7 amino acids) can be attributed to peptide molecular size.

The formation of an amino-terminated monolayer was the critical step for the synthesis of a uniformly distributed biomolecular layer. Grafting of reproducible aminoalkyl films using (aminoalkyl)trialkoxysilanes was achieved by the strict control of excess water and limiting the concentration of the silane duration of the reaction.<sup>25,61,62</sup> Moon et al.<sup>45</sup> showed that thickness and surface density of (aminoalkyl)alkoxysilanes films on silicon wafers were dependent on the incubation time in the silane solution. For (3-aminopropyl)triethoxysilane (APTES), the measured thickness using ellipsometry was ~6 Å after a 10 min deposition, compared with 50–100 Å following a 24 h incubation.<sup>45</sup> Xiao et al.<sup>31</sup> observed similar thickness of APTES films deposited on titanium from a dry toluene reflux. In our work and that of Stenger et al.,<sup>39</sup> excess water was controlled by using anhydrous methanol and subsequently adding water to limit the duration of the reaction (5 min). Polycondensation of the trialkoxysilane was minimized by slowing the rate of hydrolysis of the alkoxy groups to silanols by matching the solvent (methanol) with the leaving group for the reaction. The combination of dilute silane concentrations,<sup>16</sup> control of excess water,<sup>61</sup> solvent selection, and short deposition times yielded uniformly distributed reaction-site limited monolayers with (aminoalkyl)alkoxysilanes amenable to further synthetic modification. The quality and density of the aminosilane film allowed immobilization of peptide ligands with surface densities up to 4 pmol/cm<sup>2</sup>. Peptide surface densities higher than this range can be achieved by a combination of using multilayer siloxane films and molecules with lower molecular weight.<sup>31,32</sup> Although the peptide surface density in this work was 2 orders of magnitude lower than that of the aminosilane film, it was at least 3 orders of magnitude higher than that needed to promote cell adhesion and spreading<sup>63</sup> and proved more than sufficient to control the biological activity of attached mammalian cells in our work (see below).<sup>22,34,64</sup>

#### Effect of RGD Surface Density on Cell Attachment.

The surface density of adsorbed extracellular matrix proteins affects mammalian cell adhesion, the speed of cell migration, degree of cell spreading, and cytoskeleton

(57) Kallury, K. M. R.; Macdonald, P. M.; Thompson, M. *Langmuir* **1994**, *10*, 492–499.

(58) Trems, P.; Denoyel, R. *Langmuir* **1996**, *12*, 2781–2784.

(59) Vrancken, K. C.; Van Der Voort, P.; Possemiers, K.; Vansant, E. F. *J. Colloid Interface Sci.* **1995**, *174*, 86–91.

(60) Kruth, D. G.; Bein, T. *Langmuir* **1993**, *9*, 2965–2973.

(61) Denoyel, R.; Trems, P. *J. Phys. Chem.* **1995**, *99*, 3711–3714.

(62) Vrancken, K. C.; Coster, L. D.; Van Der Voort, P.; Grobet, P. J.; Vansant, E. F. *J. Colloid Interface Sci.* **1995**, *170*, 71–77.

(63) Massia, S. P.; Hubbell, J. A. *J. Cell Biol.* **1991**, *114*, 1089–1100.

(64) Rezanian, A.; Healy, K. E. *J. Orthop. Res.* **1999**, in press.

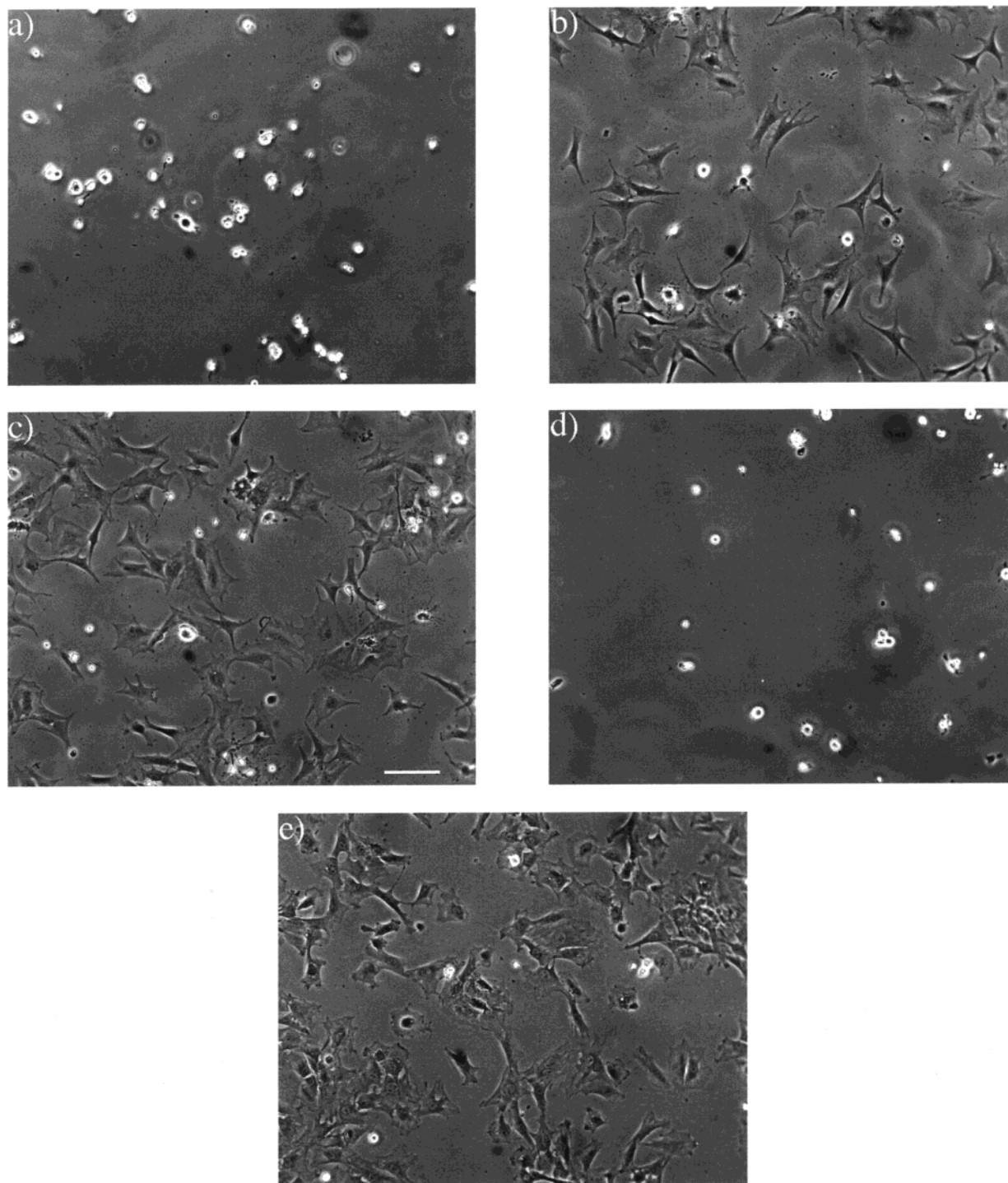


**Figure 6.** Phase contrast microscopy images of ROC cells on  $0.01 \text{ pmol/cm}^2$  -RGD- (a),  $0.62 \text{ pmol/cm}^2$  -RGD- (b),  $4 \text{ pmol/cm}^2$  -RGD- (c), -RGE- (d), and TCPS (e) (with 15% FBS) surfaces following 4 h of incubation in the presence of 1% BSA in DMEM. Highest degree of cell attachment and spreading was observed on TCPS- and RGD-grafted surfaces with a surface density of  $0.62 \text{ pmol/cm}^2$  or higher. Scale bar,  $100 \mu\text{m}$ .

organization,<sup>63,65–67</sup> which in turn affects the rate at which a surface is covered by cells. Therefore, the response of osteoblast-like cells to the engineered peptide surfaces (RGD and RGE), with various peptide surface densities ( $0.01$ – $4 \text{ pmol/cm}^2$ ), was examined by measuring the

(65) Burrige, K.; Fath, K.; Kelly, T.; Nuckolls, G.; Turner, C. *Annu. Rev. Cell Biol.* **1988**, *4*, 487–525.

(66) DiMilla, P. A.; Stone, J. A.; Quinn, J. A.; Albelda, S. M.; Lauffenburger, D. A. *J. Cell Biol.* **1993**, *122*, 729–737.

(67) Palecek, S. P.; Loftus, J. C.; Ginsberg, M. H.; Lauffenburger, D. A.; Horwitz, A. F. *Nature* **1997**, *385*, 537–540.

number/ $\text{cm}^2$  and the projected area of attached cells. The percent cell attachment and area of spread cells on RGD surfaces with peptide densities of  $0.01 \text{ pmol/cm}^2$  was significantly smaller compared with RGD surfaces with densities  $\geq 0.6 \text{ pmol/cm}^2$  (Table 3). The cells were more round and refractive on the RGE and  $0.01 \text{ pmol/cm}^2$  RGD surfaces compared with the spread morphology of the cells on either RGD  $\geq 0.6 \text{ pmol/cm}^2$  or tissue culture polystyrene (TCPS) surfaces with adsorbed serum proteins (Figure 6). The critical surface density for cell adhesion to RGD surfaces with different surface densities was higher than

that from previous observations, showing that a minimum RGD surface density of  $0.01 \text{ pmol/cm}^2$  was required for cell adhesion and focal contact formation.<sup>2,63</sup> However, competitive binding experiments using solution-phase RGD and RGE peptides showed that only solution-phase RGD blocked cell adhesion to RGD-grafted surfaces,<sup>34</sup> thus confirming the specificity of the cell with the peptide-modified surface. Previous studies have shown that the interaction of cells with RGD-modified surfaces or TCPS in the presence of serum proteins is primarily mediated by adsorbed vitronectin and the vitronectin receptor ( $\alpha_v\beta_3$ ) on the cell surface.<sup>63,68,69</sup> We have also observed that attachment of osteoblasts to the RGD surfaces was primarily mediated by the vitronectin receptor,<sup>64</sup> thus suggesting that the RGD signal promoted cell attachment through the vitronectin receptor. Moreover, using the same synthetic route we have shown that surfaces combining peptides containing both the cell- and heparin-binding domains of BSP (RGD and FHRRIKA) in a specific ratio (75:25 or 50:50) promoted greater spreading, strength of attachment, focal contact and cytoskeletal organization, and mineralization of the deposited extracellular matrix compared with homogeneous RGD and FHRRIKA surfaces.<sup>34</sup> Taken together, these data demonstrate the abil-

(68) Steele, J. G.; McFarland, C.; Dalton, B. A.; Johnson, G.; Evans, M. D. M.; Howlett, C. R.; Underwood, P. A. *J. Biomater. Sci., Polym. Ed.* **1993**, *5*, 245–257.

(69) Steele, J. G.; Johnson, G.; Underwood, P. A. *J. Biomed. Mater. Res.* **1992**, *26*, 861–884.

ity to control the interaction of cells with solid surfaces by modification with biological ligands that interact with cell-surface receptors.

### Conclusions

A simple three-step immobilization strategy was utilized to graft peptides to oxide surfaces. A reaction-site limited monolayer of EDS ( $\sim 0.7 \text{ nm}$ ,  $0.3 \text{ nmol/cm}^2$ ) provided a free amine on titanium and silicon oxides that was used to covalently couple peptides via a heterobifunctional cross-linker (SMCC). The thickness of the SMCC ( $\sim 0.4 \text{ nm}$ ) and peptide ( $\sim 0.4 \text{ nm}$ ) layers determined by spectroscopic ellipsometry was less than the extended chain projections for the respective layers and was attributed to a reduction in surface density for each layer. The response of mammalian cells to the peptide-modified surfaces was ligand- and surface density-specific, demonstrating that the quality of the engineered film was sufficient to control mammalian cell interactions with the surface. The immobilization scheme presented can be used to covalently link any molecule (e.g., peptides, peptoids, enzymes, antibodies, DNA, etc.) with a free thiol to silicon and titanium oxides. The method should find general use in applications where controlling either molecular or cell behavior at interfaces is important.

**Acknowledgment.** This research was supported by NIH/NIAMS R01A.R.43187

LA990024N